Electronic Supplementary Material (ESI) for Physical Chemistry Chemical Physics.

Supporting Information for:

Atomistic modelling of entropy driven phase transitions between different crystal modifications in polymers: the case of poly(3-alkylthiophenes)

Mosè Casalegno[a], Tommaso Nicolini[a,§], Antonino Famulari[a], Guido Raos[a], Riccardo Po[b], and Stefano V. Meille[a]*

[a]Dipartimento di Chimica, Materiali e Ingegneria Chimica "G. Natta", Politecnico di Milano, via Mancinelli 7, I-20131 Milano (MI), Italy.
[b]Research Center for Renewable Energies and Environment, Istituto Guido Donegani, Eni S.p.A, Via Fauser 4, I-28100 Novara (NO), Italy.
§ Present address: Laboratoire de Chimie des Polymères Organiques (LCPO), CNRS UMR 5629, Université de Bordeaux, Bordeaux INP, 16 Av. Pey-Berland, Pessac CEDEX, F-33607, France
*Corresponding author: valdo.meille@polimi.it.

Table of Contents

1. Calculated average potential energies and enthalpies per monomer at 300 K for P3BT and P3HT.

During a preliminary stage of our work, MD calculations were performed to assess the relative stabilities of form II and the experimentally determined form I model structures. For P3BT we considered form I', characterized by Arosio et al.[1], whereas for P3HT, the form I model developed by Kayunkid et al.[2] was used. As input structures, the supercells described in the text were used for form II. For P3BT form I' (*a* = 7.64 Å, *b* = 7.77 Å, chain axis, *c* = 24.97 Å) a suitable supercell (6x5x2, along the a, b, and c axes) was built, while for P3HT a 5x5x5 supercell was built starting from the published unit cells (*a* = 16.00 Å, *b* = 7.8 Å, chain axis, *c* = 7.80 Å, β = 86.40°)[2]. All simulations were performed at 300 K for 20 ns, within the NPT ensemble. The experimental input structures were equilibrated for 1 ns.
Table S1 below collects the values of total potential energy (U) and enthalpy (H), per monomer, obtained from the NPT simulations, as averages over 20 ns. For comparison purposes, we also report the corresponding values for the form I structures obtained in this work from form II structures.
For a given polymer, we confirmed in the present paper that the form II structure has lower potential energy and enthalpy per monomer, as compared to form I structures. This observation supports the idea that form II is more thermodynamically stable than form I at ambient temperature[3], and prompted us to investigate its thermal behavior.

Table S1. Comparison of average potential energies and enthalpies for P3BT and P3HT polymorphs at 300 K. Numerical values, referred to a single monomer unit, were obtained from 20-ns NPT run. Standard deviations are given in parenthesis.

System:	U [kJ/mol]	H [kJ/mol]
P3BT Form II	12.3(6)	83.7(8)
P3BT Form I[a]	22.6(10)	93.6(12)
P3BT Form I'[b]	21.1(15)	92.2(21)
P3HT Form II	25.9(7)	119.4(9)
P3HT Form I[b]	38.6(12)	132.1(14)
P3HT Form I[c]	38.3(7)	131.8(9)

[a] Values for the form I obtained from the corresponding form II after the phase transition, and relaxation at 300 K for 1 ns. [b] Values referred to the form I' model in Ref. (1). [c] Values referred to the form I model in Ref. (2), after 1 ns relaxation at 300 K.

2. MD qualitative evaluation of the "melting points" of infinitely periodic P3HT and P3BT form I and form II structural models.

With the aim of collecting additional indications about the relative stability of our structural models as a function of temperature, and to evaluate how the properties of the available P3BT and P3HT structural models compare with experiment, we performed additional exploratory MD simulations. Our immediate goal was to assess qualitatively the "melting temperatures" of relevant P3BT and P3HT infinitely periodic structural models. Due to the use of periodic boundary conditions, our "melt" is not completely isotropic, but it is rather a nematic consisting of infinitely periodic main chains aligned along the *b* axis, yet characterized by extensive 2D disorder within the *ac* plane. One of the most apparent structural features of such a "melt" is the complete loss of chain stacking and layering, present in both form I and form II starting structures. This loss of stacking order was chosen as criterion to assess the disordering of the structure. During the explorative simulations (limited to a maximum of 20 ns) we monitored the average distance between the projection of the center of mass of nearest neighbor polymer chains on the *a*-*c* plane.

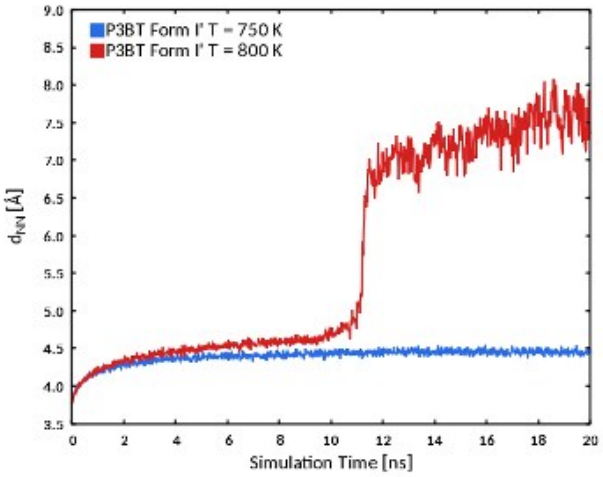

Figure S1. Plots of d_{NN} for P3BT form I' at 750 K and 800 K, as a function of the simulation time, obtained during the 20-ns NPT runs.

At a given temperature, this distance, d_{NN}, corresponds to the average stacking distance for the 50 chains present in the examined supercells, in structures where stacking order is preserved. Since both form I and form II are stacked structures this value is expected to suddenly increase approaching "melting", due to the loss of 2D structural order. Figure S1 shows the plots of d_{NN} obtained for P3BT form I' at 750 K and 800 K. The steep increase in d_{NN} value, observed at 800 K, is clearly visible, indicating form I' melting.
The MD calculations were performed starting from structures equilibrated at 300 K, and at increasing temperatures, on a 50 K grid. Table S2 below lists the lowest temperatures at which transitions occur within the 20 ns simulation time. Hence the reported values are overestimated and the "actual" melting points of our models may be up to 50 K lower than the temperatures reported in Table S2.

Table S2. Melting temperature excess estimates (see text) of infinitely periodic P3HT and P3BT form I and form II structural models.

System:	Temperature [K]
P3BT Form II[a]	700
P3BT Form I'[b]	800
P3HT Form II[a]	650
P3HT Form I[c]	800

[a] The starting form II structures were in some instances recognized to evolve transiently into unstable structures with some form I features, subsequently losing stacking and layering order. [b] Values referred to the form I' model in Ref. (1). [c] Values referred to the form I model in Ref. (2), after 1 ns relaxation at 300 K.

The estimates reported in Table S2 are about 250 K above the extrapolated experimental melting points of form I and form II P3BT and P3HT polymorphs (see below). Although this discrepancy may appear large and disappointing, it should be clear that the intramolecular periodicity implied by the superlattice periodicity, even neglecting the plausible reduction of conformational freedom of the infinite main chains, substantially limits their ability to diffuse not only along the chain axis direction, but also laterally, causing disordering processes to be substantially inhibited. The shift to higher temperature of transitions involving chain displacement is therefore expected, although its extent is hardly predictable. What is encouraging on the other hand is that consistently with experiment, both in the case of P3HT and P3BT the melting point of form II is lower than for form I, even though in both cases form II is more stable a room temperature. The fact that form II P3BT has a higher melting point than from II P3HT also correctly emerges in the MD simulations, whereas for the form I polymorphs of the two polymers similar melting temperatures are predicted, which, within the adopted resolution limits may also be acceptable.

3. Experimental melting points and enthalpies for P3HT and P3BT form I and form II polymorphs.

In the following discussion, summarizing what we consider the more reliable available literature values of the thermodynamic data pertaining to P3HT and P3BT polymorphs, we recall that widely available evidence indicates that form I can range from a relatively ordered crystalline polymorph (often called form I') to a highly disordered 2D mesophase. It is hence an oversimplification to consider form I a single crystalline polymorph as we will in the following discussion and hence we cannot expect full consistency of the data. The experimental values of the melting temperature and the melting enthalpy in the first heating for carefully solution-crystallized form I materials of relatively high molecular weight P3ATs, for a number of reasons, are normally significantly larger than in successive heating cycles.
For the equilibrium melting points, in the case of P3HT values of 571 K and 389 K for form I and form II[4] respectively were estimated based on extrapolation of a sequence of highly crystalline oligomers. A somewhat lower value of 545 K was proposed subsequently for

form I P3HT in a very accurate study[5] based on polymer material, considering also crystalline size and crystallinity. For P3BT, an equilibrium melting point of 594 K for form I has been reported[6] and experimental values as high as 565 K are present in the literature[7]. For P3BT a form II-form I transition temperature as high as 432 K was measured[3] while lower values were also reported[8]. To our knowledge, no estimates of the P3BT form II equilibrium melting temperature are available although, for infinite, perfect P3BT form II crystals we can reasonably expect it to be about 450 K i.e. somewhat (20 K) higher than highest reported P3BT form II/form I transition temperature.

In the case of P3HT accurate estimations of form I and form II melting enthalpies were reported[4], based on extrapolation of fully crystalline oligomer data. The proposed value of 39 J/g[4] was reasonably corrected to 49 J/g (8.2 kJ/mol of monomer) in a study on polymeric samples which considered also crystallinities and crystal size[5] for P3HT form I. A value of 90 J/g (15 kJ/mol of monomer)[4] appears a sensible suggestion for P3HT form II melting enthalpy[4]. These data allow estimating that the form II enthalpy should be about 7 kJ/mol of monomer lower than that of form I.

On the basis of the above data the melting entropy ΔS_m of P3HT form I can be estimated to be about 14 J K^{-1} mol^{-1} of monomer while for form II a value of ΔS_m of ca. 35 J K^{-1} mol^{-1} of monomer can be suggested. The entropy of form I P3HT is substantially larger than the entropy of form II and the increase in entropy in the form II-form I transition is ca. 20 J K^{-1} mol^{-1} of monomer, significantly larger than the form I melting entropy. It is quite reasonable hence to describe form I P3HT at the transition temperature of about 370 K as a high entropy mesophase.

For P3BT form I, experimental melting enthalpies of 26 J/g (3.6 kJ/mol of monomer)[1] and 29 J/g (4.0 kJ/mol of monomer)[3] have been reported for polymeric samples in which crystallinity is likely to be far from 100%. In the first work[1] a sample crystallinity of 45% has been estimated by X-ray diffraction: hence a melting enthalpy of ca. 8.0 kJ/mol of monomer can be estimated for a fully crystalline P3BT form I sample. The same value is obtained assuming a crystallinity of 50% in second study[3]. This is quite plausible because the preparation of the sample in Ref. (3) is identical to the one reported in Ref. (9) were a crystallinity of 50% was determined, from X-ray diffraction. The enthalpy associated with the melting/recrystallization of form II into form I is found[3] to be 19 J/g (2.6 kJ/mol per monomer), which assuming a crystallinity of 50%, must be corrected to 5.2 kJ/mol per monomer.

The melting entropy ΔS_m of P3BT form I can be estimated to be about 14 J K^{-1} mol^{-1} of monomer while for form II a value of ΔS_m of ca. 26 J K^{-1} mol^{-1} of monomer can be suggested. Again the entropy of form I P3BT is substantially larger than the entropy of form II and the increase in entropy in the form II-form I transition is ca. 12 J K^{-1} mol^{-1} of monomer, approaching the form I melting entropy.

The above estimates of the form I-form II enthalpy differences for the two polymers are reasonably comparable with the values that can be extracted from Table S1, namely about 10 kJ/mol for P3BT and 13 kJ/mol for P3HT. The differences may be due to a number of factors, relating to experimental uncertainties, force-field imperfections, the use of periodic boundary conditions in our MD simulations, etc.. The reasons why we describe the form II-form I transition as entropy driven should however be clear, as well as why the form I polymorphs at the transition temperature and above are legitimately described as mesophases.

4. Comparison of Form II unit cell parameters for P3BT and P3HT and force-field validation.

Table S3 collects the lattice parameters of form II for P3BT and P3HT, as obtained from the NPT (20 ns) simulations performed at 300 K. For comparison purposes, we also reported the same parameters as found in the literature for P3BT[9] and P3HT[10], where available. For P3HT, we considered the P3HT-26 molecules, with an average molecular weight of 26400 g/mol. The layer periodicity, d_{100}, and the spacing between adjacent thiophene rings (π-π stackings) within a given stack, d_{002}, were also reported. The latter was calculated along the c axis, given that we preferred to take the *b* axis as the main chain axis.

For P3BT, the change in lattice parameters was less than 1% while a difference of 3.8° for the β angle results. The values of d_{100} and d_{002} were also consistent with those previously reported[9].

For P3HT, the MD simulations confirmed the reliability of the initial energy-minimized structure. Our final values of a and c (13.28 Å and 9.35 Å) agree well with those obtained in SAED experiments (13.1 Å and 9.3 Å, respectively)[10]. The inter-layer distance of the relaxed structure, d_{100} = 12.63 Å, is comparable with the value of 12 Å commonly reported in the literature[11,12,13]. For the intra-layer distance, our estimate, d_{002} = 4.44(1) Å, is close to the experimental value of 4.4 Å, as determined in SAED[10] and XRD[12] experiments.

Table S3. Comparison of form II unit cell parameters for P3BT and P3HT. Inter-layer distances (d_{100}), π-π stackings (d_{002}), and densities are also reported. Standard deviations are given in parenthesis.

System:	a [Å]	b [Å]	c [Å]	β [°]	d_{100} [Å]	d_{002} [Å]	Density [g/l]
P3BT unit cell[a]	10.76	7.77	9.44	64.66	9.72	4.26	1290.0
P3BT MD 300K	10.836(1)	7.807(5)	9.358(1)	68.26(1)	10.066(1)	4.34(1)	1304.5(1)
P3HT unit cell[b]	13.1(5)	7.80[d]	9.24(50)[c]	68.5(5)[c]	---	4.3	---
P3HT MD 300K	13.286(2)	7.814(1)	9.353(2)	71.98(3)	12.630(1)	4.44(1)	1197.3(1)

[a] Values from Ref. (9). [b]Values referred to P3HT-26 in Ref.(10). [c] Consistently with our choice of the *b* axis as the main chain axis, the lattice was appropriately modified. [d] Not reported in Ref. (10), and set equal to that of our unit cell.

5. Movie of P3HT phase transition.

A 25 s video illustrating the P3HT phase transition (first 20 ns) observed at 530 K has been prepared using VMD[14] and is available in AVI format.

6. P3BT and P3HT sample preparation and XRD measurements.

P3BT samples are those prepared as described in Ref. (1). Samples were enclosed in 0.7 mm glass capillaries. High temperature WAXD patterns (Cu-Kα) were collected in transmission geometry by means of a Bruker P4 diffractometer equipped with a Hi-Star 2D detector. Background WAXS (including capillary contributions) were subtracted from each diffraction pattern. Sample temperatures were controlled with an in-house equipment based on a hot air device with a thermocouple.
P3HT samples with Mn = 20 kDa and RR-97% were used for the preparation of solid mixtures with trichlorobenzene (TCB) (composition 4:100 w/w) according to the procedure described in Ref. (2). After TCB sublimation under vacuum, spherical polycrystalline aggregates (diameter ≈ 0.1 mm) were obtained and mounted on a fiber to record room temperature 2D patterns on Bruker P4 diffractometer (Cu-Kα) using an imaging plate detector. Data were collected at different 2θ diffractometer angles, with the sample rotating around ϕ, and 2D patterns were corrected for centering and detector shape with the XRD2D 80 software and merged. Integration over χ at constant 2θ was then performed to obtain 1D PWD-XRD patterns.
The adopted data collection procedures on the Bruker P4 diffractometer have been shown[1,9] to yield diffraction patterns closely approaching those obtained with random crystallite orientations.

7. Calculation of the XRD diffraction patterns.

The calculation of the powder diffraction patterns shown in Figures 5 and 6 (see main text), was addressed with an in-house program developed by our group. The atomic scattering factors were calculated at λ = 1.5418 Å, and corrected for the effect of temperature via a isotropic, Debye-Waller factor ($B = 8\pi^2U$), with U = 0.05 Å^2. The signal intensity was corrected for Lorentz-polarization, while the effects of absorption were neglected. No background was included. Plane multiplicity and preferred orientation were not explicitly taken into account. For peak profiles Lorentzian functions were adopted, assuming for simplicity a value of 1° (2θ) for the full width at half maximum in all diffraction patterns. The program's reliability was successfully tested against the powder diffraction spectra generated by Mercury (v. 3.8)[15], for different P3AT structures. Using the same input parameters, we found the patterns of our program to match those obtained from Mercury. Minor differences were found in peak intensity, due to the use of different profile functions (symmetric pseudo-Voight) in Mercury.

8. Details of MD simulations.

All MD simulations for both P3BT and P3HT were carried out were performed with the package GROMACS 5.0.4.[16], at constant temperature and pressure, thus within the NPT ensemble. The leapfrog algorithm with a time step of 1 fs was used to integrate the equations of motion. As stated in the main text, the temperatures were varied in order to find the phase transition temperature. The temperature was controlled by coupling with a velocity rescaling thermostat[17], with a time constant of 0.5 ps. The pressure was maintained constant (1 bar) and controlled via anisotropic coupling to the Berendsen barostat[18], with a coupling constant of 5.0 ps. The Berendsen, rather than the more accurate Parrinello-Rahman barostat[19] was chosen after some numerical tests, because of its better numerical stability. The compressibility was set to 10^{-6} bar^{-1}. Periodic boundary conditions were applied along all dimensions. All short-range nonbonded interactions were cutoff at 1.2 nm. Electrostatic interactions were treated via the particle-mesh-Ewald method[20] with a Fourier grid spacing of 0.12 nm. Hydrogen atoms were treated explicitly with no constraints. The neighbor list was updated every 10 steps, and buffered according to the Verlet scheme.
The FF3 force filed parameters used in this work are available in the Supplementary Information of Ref. [21].

9. Complementary results from the MD simulations of P3BT and P3HT phase transitions.

Figure S2 shows the evolution of the unit cell parameters *a*, *b*, and *c*, and densities of both P3BT and P3HT during the form II-form I phase transitions, observed at 560 K and 530 K, respectively. The change in these parameters is consistent with the snapshots reported in the main text (e.g. Figure 3 and 4).
For P3HT, the phase transition involved the expansion of the box mostly along the "lamellar" *a* axis. The change along this axis was characterized by a sharp transition starting at 12 ns. The *c* axis gradually increased from the beginning of the simulation, up to 12 ns, when a sudden change, similar to that observed for *a*, occurred. Consistently with the snapshot reported in Figure 3 (frames B and C), the main change in these parameters elapsed in about 5 ns. After the transition, no substantial change in *a* was observed, while c further increased during the rest of the simulation. The change in density followed a similar behavior, characterized by a gradual change in the interval 0-12 ns, followed by a steep decrease during the phase transition. A slight decrease in *b* also occurred, corresponding to the shortening of the box along the main chain axis.
For P3BT, the phase transition mostly involved a gradual change in *c*, whereas *a* and *b* did not changed appreciably. The change in density was specular to that in *c*. Overall, the transition took about 18 ns to complete, starting at the beginning of the simulation, with a relatively gradual evolution, in contrast to that of P3HT.

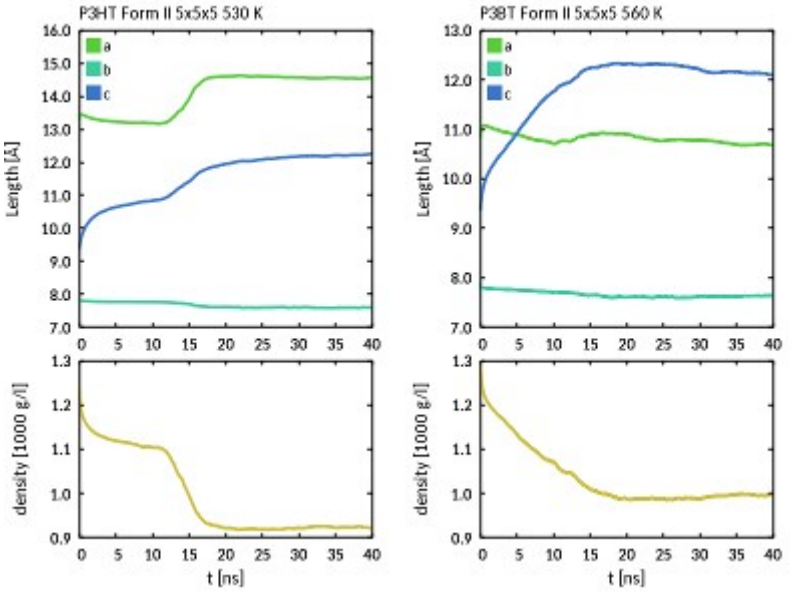

Figure S2. Evolution of the unit cell parameters a, b, and c for P3BT (top left) and P3HT (top right) for the MD simulations describing the phase transitions form II-form I. The bottom panels report the evolution of the corresponding densities during the dynamics.

References

1 P. Arosio, M. Moreno, A. Famulari, G. Raos, M. Catellani, and S. V. Meille, *Chem. Mater.* **2009**, *21*, 78-87.
2 N. Kayunkid, S. Uttiya, and M. Brinkmann, *Macromolecules* **2010**, *43*, 4961-4967.
3 G. Lu, L. Li, and X. Yang, *Macromolecules* **2008**, *41*, 2062-2070.
4 F. P. V. Koch, M. Heeney, and P. Smith, *J. Am. Chem. Soc.* **2013**, *135*, 13699-13709.
5 C. R. Snyder, R. C. Nieuwendaal, D. M. DeLongchamp, C. K. Luscombe, P. Sista, and S. D. Boyd, *Macromolecules* **2014**, *47*, 3942-3950.
6 V. Causin, C. Marega, A. Marigo, L. Valentini, and J. M. Kenny, *Macromolecules* **2005**, *38*, 409-415.
7 S. Li, S. Wang, B. Zhang, F. Ye, H. Tang, Z. Chen, and X. Yang, *Org. Electron.* **2014**, *15*, 414-427.
8 Y. Yuan, Y. Zhang, X. Cui, and J. Zhang, *Polymer* **2016**, *105*, 88-95.
9 Buono, N. H. Son, G. Raos, L. Gila, A. Cominetti, M. Catellani, and S. V. Meille, *Macromolecules* **2010**, *43*, 6772-6781.
10 K. Rahimi, I. Botiz, N. Stingelin, N. Kayunkid, M. Sommer, F. P. V. Koch, H. Nguyen, O. Coulembier, P. Dubois, M. Brinkmann, and G. Reiter, *Angew. Chem. Int. Ed.* **2012**, *51*, 11131-11135.
11 S. Joshi, S. Grigorian, U. Pietsch, *Phys. Stat. Sol.,* **2008**, *205*, 488-496.
12 Zen, M. Saphiannikova, D. Neher, J. Grenzer, S. Grigorian, U. Pietsch, U. Asawapirom, S. Janietz, U. Scherf, I. Lieberwirth, and G. Wegner, *Macromolecules* **2006**, *39*, 2162-2171.
13 S. V. Meille, V. Romita, T. Caronna, A. J. Lovinger, M. Catellani, and L. Belobrzeckaja, *Macromolecules* **1997**, *30*, 7898-7905.
14 W. Humphrey, A. Dalke, and K. J. Schulten, *Mol. Graph.* **1996**, *14*, 33-38.
15 F. Macrae, I. J. Bruno, J. A. Chisholm, P. R. Edgington, P. McCabe, E. Pidcock, L. Rodriguez-Monge, R. Taylor, J. Van De Streek, and P. A. Wood, *J. Appl. Cryst.* **2008**, *41*, 466-470.
16 B. Hess, C. Kutzner, D. van der Spoel, and E. J. Lindahl, *Chem. Theory Comput.* **2008**, *4*, 435-447.
17 G. Bussi, D. Donadio, and M. Parrinello, *J. Chem. Phys.* **2007**, *126*, 014101.
18 H. J. C. Berendsen, J. P. M. Postma, W. F. van Gunsteren, A. DiNola, and J. R. J. Haak, *Chem. Phys.* **1984**, *81*, 3684-3690.
19 M. Parrinello, and A. Rahman, *J. Appl. Phys.* **1981**, *52*, 7182-7190.
20 T. Darden, D. York, and L. Pedersen, *J. Chem. Phys.* **1993**, *98*, 10089-10092.
21 M. Moreno, M. Casalegno, G. Raos, S. V. Meille, and R. Po, *J. Phys. Chem. B* **2010**, *114*, 1591-1602.